© 2017. Published by The Company of Biologists Ltd | Development (2017) 144, 731 doi:10.1242/dev.149567

CORRECTION

Correction: Foxn4 promotes gene expression required for the formation of multiple motile cilia

Evan P. Campbell, Ian K. Quigley and Chris Kintner

There was an error published in Development **143**, 4654-4664.

The name of the first author was misspelt. The correct name appears above and has been corrected in the published article.

The authors apologise to readers for this mistake.

© 2016. Published by The Company of Biologists Ltd | Development (2016) 143, 4654-4664 doi:10.1242/dev.143859

RESEARCH ARTICLE

Foxn4 promotes gene expression required for the formation of multiple motile cilia

Evan P. Campbell*, Ian K. Quigley* and Chris Kintner‡

ABSTRACT

Multiciliated cell (MCC) differentiation involves extensive organelle biogenesis required to extend hundreds of motile cilia. Key transcriptional regulators known to drive the gene expression required for this organelle biogenesis are activated by the related coiled-coil proteins Multicilin and Gemc1. Here we identify *foxn4* as a new downstream target of Multicilin required for MCC differentiation in *Xenopus* skin. When Foxn4 activity is inhibited in *Xenopus* embryos, MCCs show transient ciliogenesis defects similar to those seen in mutants of Foxj1, a known key regulator of genes required for motile ciliation. RNAseq analysis indicates that Foxn4 co-activates some Foxj1 target genes strongly and many Foxj1 targets weakly. ChIPseq suggests that whereas Foxn4 and Foxj1 frequently bind to different targets at distal enhancers, they largely bind together at MCC gene promoters. Consistent with this co-regulation, cilia extension by MCCs is more severely compromised in *foxn4* and *foxj1* double mutants than in single mutants. In contrast to Foxj1, Foxn4 is not required to extend a single motile cilium by cells involved in left-right patterning. These results indicate that Foxn4 complements Foxj1 transcriptionally during MCC differentiation, thereby shaping the levels of gene expression required for the timely and complete biogenesis of multiple motile cilia.

KEY WORDS: Cilia, Foxj1, Foxn4, Multiciliate cells, *Xenopus laevis*

INTRODUCTION

The multiciliated cell (MCC) is a specialized epithelial cell type that employs hundreds of motile cilia in order to produce robust fluid flow along lumenal surfaces (Brooks and Wallingford, 2014). To undergo multiple motile ciliation, MCC differentiation requires substantial changes in gene expression that enable large numbers of complex organelles to form (Quigley and Kintner, 2016 preprint). Analysis of this gene expression can provide insights into the macromolecular complexes required for cilia assembly and function, as well as into how motile cilia are impaired in human ciliopathies such as primary ciliary dyskinesia (PCD) (Choksi et al., 2014).

Two related coiled-coil proteins, Multicilin and Gemc1, are both necessary and sufficient to initiate MCC differentiation, acting as co-regulators in a transcriptional complex with a subset of the E2F proteins (Arbi et al., 2016; Kyrousi et al., 2015; Ma et al., 2014; Stubbs et al., 2012; Terre et al., 2016; Zhou et al., 2015). The complex between Multicilin, E2f4 and DP1 (EDM) in particular appears to directly activate gene expression required for centriolar biogenesis (Ma et al., 2014), thus driving a novel form of organelle assembly that enables MCCs to form the hundreds of basal bodies required for multiple ciliation. Multicilin and Gemc1 also initiate gene expression required for motile cilium formation during MCC differentiation, but this occurs indirectly via their ability to activate the expression of Foxj1, a key regulator of genes required for motile axoneme extension in combination with the Rfx factors (Choksi et al., 2014). Foxj1 is also required to induce a single motile cilium to form on cells located within a structure called the left-right organizer (LRO) in the early embryo (Brody et al., 2000; Stubbs et al., 2008). Thus, one transcriptional program (predominantly dependent on Foxj1) is required for motile cilium biogenesis regardless of whether this program operates in cells with one or many cilia, while a second transcriptional program (predominantly dependent on Gemc1/Multicilin) is required specifically in MCCs for centriole biogenesis to increase cilia number.

Current models do not fully explain how an MCC is capable of forming hundreds of motile cilia, not just the one cilium that Foxj1 induces at the LRO. Biogenesis of cilia can be sensitive to the levels of transcriptional activity driving cilia gene expression. For example, the length of cilia ectopically induced by Foxj1 is dependent on the levels of Foxj1 ectopically expressed (Stubbs et al., 2008). In addition, especially broad transcriptional activity may be required to drive the relatively large number of genes upregulated during MCC differentiation. For example, ∼800 genes are markedly upregulated in differentiating MCCs, whereas ∼150 genes are upregulated in skin ionocytes, based on extensive RNAseq analysis of *Xenopus* skin progenitors (Quigley and Kintner, 2016 preprint). Thus, gene expression required for multiple cilia formation might require high levels of Foxj1 and Rfx factor expression, uniquely driven to these levels in MCCs by Multicilin/Gemc1, acting directly or perhaps indirectly via Tp73 (Nemajerova et al., 2016). Alternatively, Multicilin/Gemc1 could facilitate Foxj1 action in MCCs by activating additional regulators. One precedent for the latter possibility is that Multicilin activates the expression of Myb, which is clearly required for MCC differentiation in the lung (Tan et al., 2013). However, Myb targets and mechanism of action during MCC differentiation remain unclear, especially in light of the finding that it is also required for the differentiation of other lung cell types (Pan et al., 2014). Thus, additional regulators downstream of Multicilin/Gemc1 might be required to shape gene expression during MCC differentiation, in order to produce the relatively broad and high-level gene expression required for multiple motile cilia to form.

Here we identify and characterize *foxn4*, which encodes another forkhead transcription factor, as a gene strongly upregulated during MCC differentiation in the *Xenopus* larval skin. Although Foxn4 expression occurs in MCC progenitors in the mouse lung, the analysis of conditional *Foxn4* mutants failed to detect a gross MCC

Molecular Neurobiology Laboratory, The Salk Institute for Biological Studies, La Jolla, CA 92037, USA.
*These authors contributed equally to this work

‡Author for correspondence (kintner@salk.edu)

C.K., 0000-0002-8288-0296

Received 17 August 2016; Accepted 27 October 2016

Development (2016) 143, 4654-4664 doi:10.1242/dev.143859

phenotype (Hoh et al., 2012; Li and Xiang, 2011; Treutlein et al., 2014). We nonetheless examined Foxn4 function further in *Xenopus* skin MCCs, using both morpholino knockdown and Cas9/CRISPR mutagenesis. Both approaches produce the same phenotype, in which MCCs initiate centriole biogenesis but then show defects in basal body docking and cilia extension, similar to the defects observed in *foxj1* mutants. This cilia extension phenotype, mostly, but not completely, recovers over time, resulting in a marked subset of MCCs that are not fully differentiated. The RNAseq analysis of mutant phenotypes and the ChIPseq analysis of Foxn4 binding suggest that Foxn4 is present at MCC gene promoters, where it regulates a subset of Foxj1 transcriptional targets strongly and many Foxj1-regulated genes weakly. Consistent with this co-regulation, disrupting both Foxn4 and Foxj1 with Cas9/CRISPR leads to an even more extreme phenotype than that observed when each is targeted alone. Finally, we show that Foxn4 is apparently not required for motile cilia formation in the *Xenopus* LRO, where Foxj1, by contrast, plays a crucial role. Together, these findings indicate that Foxn4 functions to ensure robust gene expression during MCC differentiation, thus allowing large numbers of specialized organelles to be assembled in a timely fashion.

RESULTS

Foxn4 expression is activated during MCC differentiation

A timecourse study using RNAseq was previously carried out on skin progenitors in *Xenopus* (Quigley and Kintner, 2016 preprint) in which Notch signaling and/or Multicilin activity was perturbed. Both *foxn4* homeologs encoded in the pseudotetraploid *Xenopus laevis* genome, namely *foxn4.l* and *foxn4.s* (Session et al., 2016), markedly changed in levels in these datasets in a manner associated with MCC formation (Fig. S1A). Both *foxn4* homeologs responded rapidly to Multicilin activation (within 3 h; data not shown) and both were downregulated in progenitors expressing the E2f4 mutant E2f4ΔCT, which disrupts gene expression that is largely dependent on the EDM complex (Fig. S1A) (Ma et al., 2014). Consistent with direct regulation by the EDM complex, ChIPseq analyses showed strong binding of E2f4 at the proximal promoter of both *foxn4* homeologs, in a manner that is enhanced in the presence of Multicilin (Ma et al., 2014), whereas the binding of other regulators such as Foxj1 and Rfx2 was less pronounced (Fig. S1B) (Quigley and Kintner, 2016 preprint) (Chung et al., 2014).

These data suggest that *Xenopus foxn4* is an early target of the EDM complex, as compared with other transcription factors associated with MCC differentiation such as *foxj1* and *rfx2*. Moreover, a survey of the literature indicates that *Foxn4* expression is also strongly associated with MCC differentiation in the mouse: antibody staining detects transient expression of Foxn4 in progenitors during lung development (Li and Xiang, 2011) and RNA profiling consistently finds a marked increase in *Foxn4* RNA expression in MCC progenitors (Hoh et al., 2012; Treutlein et al., 2014). Thus, upregulation of *foxn4* by Multicilin acting through the EDM complex is likely to be a conserved event during early MCC differentiation in different organs and species.

A Foxn4 morpholino delays basal body docking and cilia extension

To determine whether Foxn4 contributes to MCC differentiation, we injected *Xenopus* embryos with a Foxn4 morpholino targeting the translation start site (Table S1). Cell type specification in Foxn4 morphants appeared largely normal, but when MCCs were assessed at stage 26, their differentiation was severely perturbed in that cilia number and length were dramatically reduced (Fig. 1A,B). Differentiating MCCs in Foxn4 morphants initiated centriole assembly, based on markers such as GFP-tagged forms of Centrin4, Chibby, Tsga10 and Clamp, but most of these centriolar structures failed to dock at the apical surface as basal bodies and mediate axonemal extension (Fig. 1D-G, Fig. S2). Hyls1-GFP, another centriolar marker (Dammermann et al., 2009), was strongly reduced during basal body formation in Foxn4 morphant MCCs, but retained at centrioles, further suggesting that these MCCs are deficient in basal body maturation (Fig. 1B). Significantly, MCCs in Foxn4 morphants typically extended just one or two cilia initially, presumably by employing pre-existing centrioles as basal bodies (labeled with Hyls1-GFP, Fig. 1B, arrow). This phenotype suggests that cilia extension can occur in Foxn4 morphant MCCs with a similar timecourse as in wild-type MCCs, but is limited due to defects in the pathways leading from centriole biogenesis to basal body docking and function.

Since MCC differentiation in the *Xenopus* skin is highly synchronized, we examined different developmental stages to assess the severity of the phenotype over time. In control embryos, the number of basal bodies positioned near the apical surface has already plateaued by stage 26 (Fig. 1J), and cilia extension is almost complete (Fig. 1A). By contrast, in stage 26 Foxn4 morphants, most MCCs contained centriolar structures that were still located deep in the cytoplasm, and cilia number was severely reduced (Fig. 1H,J). By stage 30, however, the number of basal bodies located apically in Foxn4 morphant MCCs was not significantly different from that in control embryos (two-tailed *t*-test, $P=0.8$), and most of these extended cilia (Fig. 1I,J). Thus, the MCCs largely recovered in the Foxn4 knockdown, even though some cells with defective cilia extension were still evident even at stage 30 (Fig. 1I). Moreover, even at this late stage, a significant number of 'normal' MCCs contained basal bodies that remained undocked, a phenotype rarely seen in controls (Fig. 1I). Thus, MCC differentiation in Foxn4 morphants recovers significantly from a severe delay, but remains incomplete.

Foxn4 activity induces ectopic cilia formation

To assess the specificity of the morphant phenotypes described above, we attempted a rescue by injecting RNA encoding a form of Foxn4 lacking the morpholino targeting sequence. Since overexpressing Foxn4 in the early embryo by RNA injection proved toxic, we engineered an inducible form of Foxn4 by fusing the ligand-binding domain of the glucocorticoid receptor to the C-terminus (Foxn4-HGR). The MCC phenotype in Foxn4 morphants at stage 26 was largely rescued by injecting *foxn4-HGR* RNA at the 2- to 4-cell stage, and treating with dexamethasone (Dex) at stage 11 (Fig. S3D), indicating that the Foxn4 phenotype is specific. In addition, in embryos injected with even higher doses of *foxn4-HGR* RNA and treated with Dex, ectopic cilia subsequently formed on outer cells, usually two per cell (Fig. S4G). Ectopic expression of the inducible Foxn4 also promoted ectopic cilia formation when embryos were co-injected with RNAs that blocked endogenous MCC differentiation (using a dominant-negative form of Multicilin, or activated Notch), indicating that Foxn4 is sufficient to drive the docking of centrioles as basal bodies and the extension of an axoneme (Fig. S4C-F).

Together, these results provide strong evidence that the basal body docking and cilia extension phenotype of Foxn4 morphants is a specific defect, and also show that these processes can by promoted ectopically in outer cells by expression of Foxn4. These results also reveal marked loss- and gain-of-function similarities in Foxn4 with those previously reported for Foxj1 in terms of a role in ciliation during MCC differentiation (Stubbs et al., 2008).

Development (2016) 143, 4654-4664 doi:10.1242/dev.143859

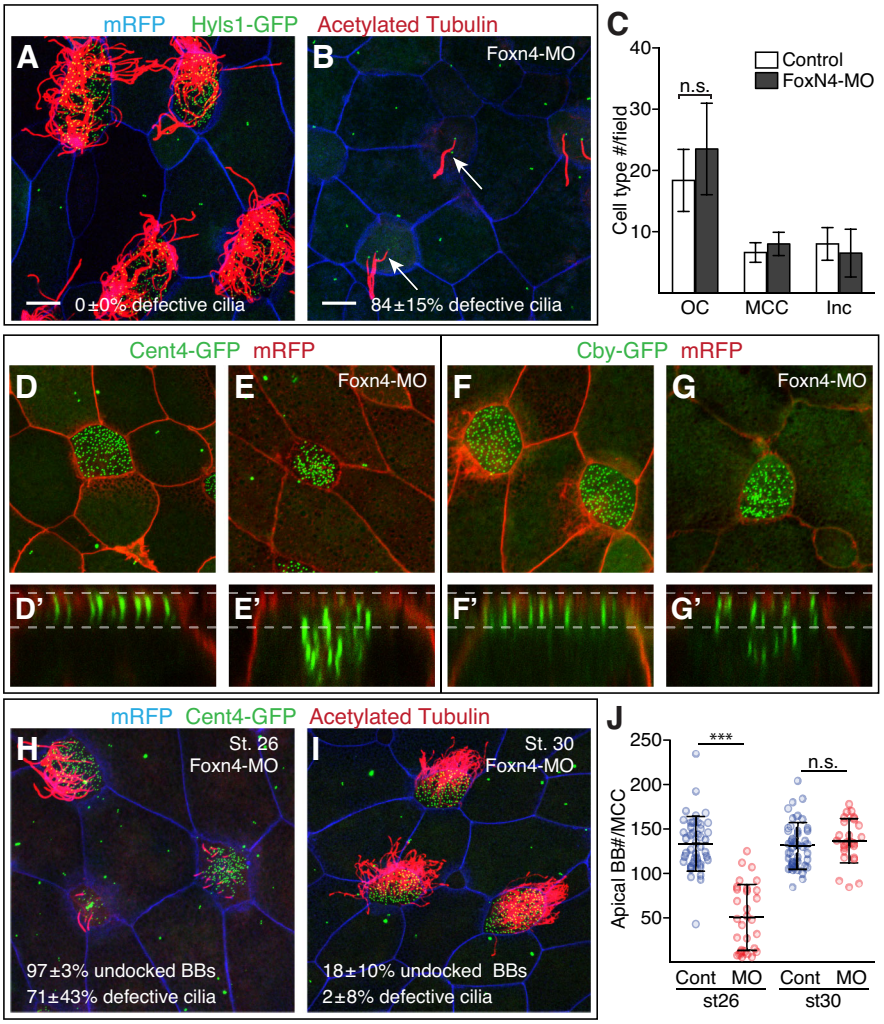

Fig. 1. MCC differentiation is disabled in Foxn4 morphants. (A-C) *Xenopus* embryos were injected at the two-cell stage with a Foxn4 morpholino, followed with RNA encoding mRFP (blue) and Hysl1-GFP (green) to label membranes and centrioles, respectively. At stage 26, embryos were fixed and cilia (red) stained with an acetylated tubulin antibody. Shown are representative confocal images of the skin in a wild-type control (A) and Foxn4 morphant (B) embryo, along with the percentage of MCCs (±s.d.) displaying defective cilia based on scoring eight fields from different embryos. Scale bars: 10 µm. (C) Plot showing the average number of MCCs (based on cilia extension), outer cells (OC) and putative ionocytes (Inc) in a 0.13×0.13 mm field of the skin, based on data from eight or nine stage 26 embryos. Error bars indicate s.d. (D-G) Confocal images of the skin in control (D,F) or Foxn4 morphants (E,G) at stage 26, where basal bodies are marked by expression of Centrin4-GFP (green, D,E) or Chibby-GFP (green, F,G) and cell boundaries with mRFP. (D-G′) Below each image is a *z*-scan, where the apical surface and basal body positions in wild-type embryos are marked by the upper and lower dashed lines, respectively. (H,I) Confocal images of the skin in Foxn4 morphants, where cell boundaries are labeled with mRFP (blue), basal bodies with Centrin4-GFP (green), and cilia by acetylated tubulin immunostaining (red), fixed at stage 26 (H) and stage 30 (I), along with the percentage of MCCs (±s.d.) with undocked basal bodies or defective cilia extension obtained by scoring at least eight fields from different embryos. In wild-type controls, MCCs with these phenotypes were rarely observed. (J) Scatter plot of basal body number located within 1 µm of the apical surface in wild-type MCCs or those in Foxn4 morphants at the indicated stages. The central bar indicates the mean and error bars indicate s.d. ***P<0.001; n.s., not significant.

foxn4 Cas9/CRISPR mutagenesis produces phenotypes that recapitulate those of Foxn4 morphants

Recent work in zebrafish has raised significant concerns about using morpholinos to assess gene function (Kok et al., 2015). To address these concerns, we asked whether similar Foxn4 phenotypes also occurred in F0 *Xenopus* embryos when targeted mutations were generated in the *foxn4* genes using Cas9/CRISPR (Bhattacharya et al., 2015; Guo et al., 2014). Two independent gRNAs were designed that target conserved sequences encoding the forkhead domain within the third exon of all four *foxn4* alleles in the pseudotetraploid *X. laevis* genome (Session et al., 2016). Each gRNA was injected separately within 40 min after fertilization along with the Cas9 protein (see Materials and Methods), and MCC differentiation was assessed at both stage 26 and stage 30 as above. Injection of Foxn4^{gRNA1} resulted in embryos in which skin cell fate was apparently unchanged, but again where a large fraction of MCCs (~80%) showed the exact same phenotype as observed in Foxn4 morphants: a majority of the basal bodies were undocked apically and cilia extension was largely depleted, except for a few short cilia (Fig. 2A-C). A second Foxn4 gRNA produced the same MCC phenotype with a lower penetrance (Fig. 2C). Significantly, the MCC phenotype generated by *foxn4* Cas9/CRISPR observed at stage 26 largely recovered by stage 30 (Fig. 2D-F). Thus, the severity and timing of the phenotype provides further evidence that MCC differentiation is markedly delayed, mostly recovers, but is still incomplete in the absence of Foxn4.

Comparison of Foxn4 and Foxj1 phenotypes

The basal body docking phenotype observed in Foxn4 knockdowns resembles those observed in *Xenopus* Foxj1 morphants or mouse *Foxj1* mutants (Brody et al., 2000; Stubbs et al., 2008). To examine this similarity further, we generated *foxj1* mutants by injecting embryos with Cas9 and a gRNA targeting a sequence encoding the forkhead domain in all four alleles in the *X. laevis* genome. MCC fate was established normally in embryos injected with Cas9/Foxj1^{gRNA1} (Fig. 3A,C), but ~80% of the MCCs were arrested in their differentiation, with multiple undocked centrioles and poor cilia extension (Fig. 3D), as described previously in Foxj1 morphants (Stubbs et al., 2008). The MCCs in *foxj1* mutants were at least as defective as those in *foxn4* mutants at stage 26 (data not shown) and, by contrast, showed little recovery in that they extended only a few short cilia when examined as far as stage 32 (Fig. 3B). Moreover, in contrast to the *foxn4* mutants that developed normally into tadpoles, based on gross morphology the *foxj1* mutants developed severe edema at swimming tadpole stages and left-right patterning defects, consistent with the known role of Foxj1 in forming the ciliated nephrostomes of the kidney and the LRO (data not shown) (Stubbs et al., 2008).

The phenotypes described above indicate that Foxn4, along with Foxj1, is upregulated by Multicilin to promote organelle biogenesis during MCC differentiation. To test this hypothesis further, we examined whether Foxn4 acts downstream of Multicilin. The expression and activation of an inducible Multicilin at stage 11 is

Development (2016) 143, 4654-4664 doi:10.1242/dev.143859

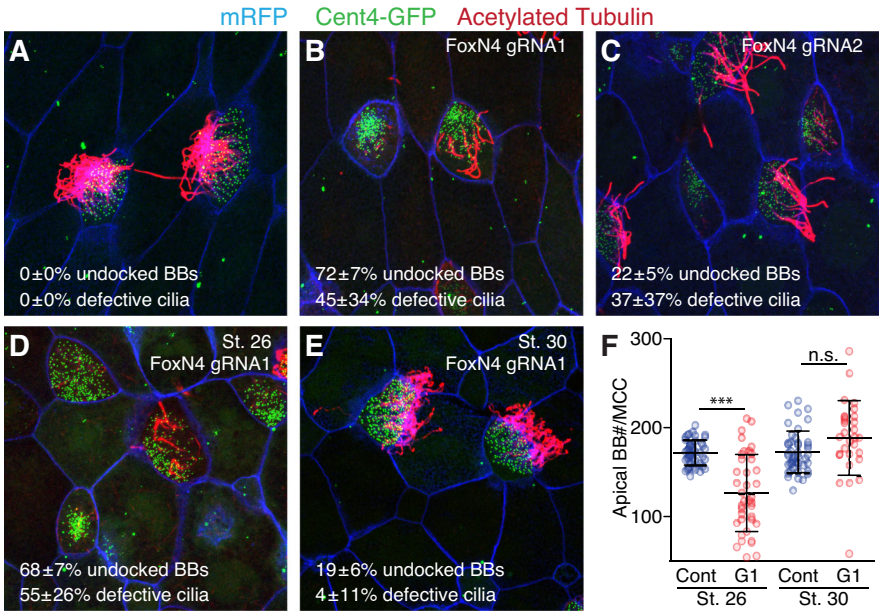

Fig. 2. *foxn4* Cas9/CRISPR phenotypes. (A-C) Representative confocal images of the skin in stage 26 wild-type control embryos (A) or embryos injected with Cas9 along with two independent gRNAs directed against *foxn4* (B,C). Cell membranes (mRFP, blue), basal bodies (Centrin4-GFP, green) and cilia (acetylated tubulin, red) are labeled as in Fig. 1. (D,E) Representative confocal images of the skin of embryos at stage 26 or stage 30, following injection with Cas9 protein and Foxn4^{gRNA1}. Cell boundaries (blue), basal bodies (green) and cilia (red) are labeled as above. (A-E) The percentage of MCCs (±s.d.) with defective cilia or undocked basal bodies is indicated based on scoring at least 12 fields from different embryos (n≥50 cells). (F) Scatter plot of basal body number located within 1 µm of the apical surface in MCCs of wild-type controls (blue, Cont) and Cas9/Foxn4^{gRNA1}-injected embryos (red, G1) at the indicated stages. The central bar indicates the mean and error bars indicate s.d. ***P<0.001; n.s., not significant.

sufficient to convert essentially all skin cells into MCCs (Fig. 3E). When inducible Multicilin is expressed in embryos injected with Cas9 along with Foxn4^{gRNA1} or Foxj1^{gRNA1}, MCC differentiation was severely disrupted in a similar way (Fig. 3F,G). In both mutant backgrounds, the MCCs induced by Multicilin initiated centriole biogenesis but were defective in docking these as basal bodies at the apical surface (Fig. 3H) and in extending cilia (Fig. 3E-G). Again, the Foxj1 and Foxn4 phenotypes produced in the presence of Multicilin resembled that produced by morpholino knockdown (Stubbs et al., 2008) (Fig. S5), although with less penetrance, since ~20% of the cells appeared normal in the nuclease-induced mutations, consistent with a clonal mixture of null mutants and wild-type escapers (Fig. 3H). Thus, these results independently confirm Foxj1 function in MCCs in *Xenopus* skin, highlight the efficacy of Cas9/CRISPR mutagenesis, indicate that Foxn4, like Foxj1, acts downstream of Multicilin, and emphasize the similarity

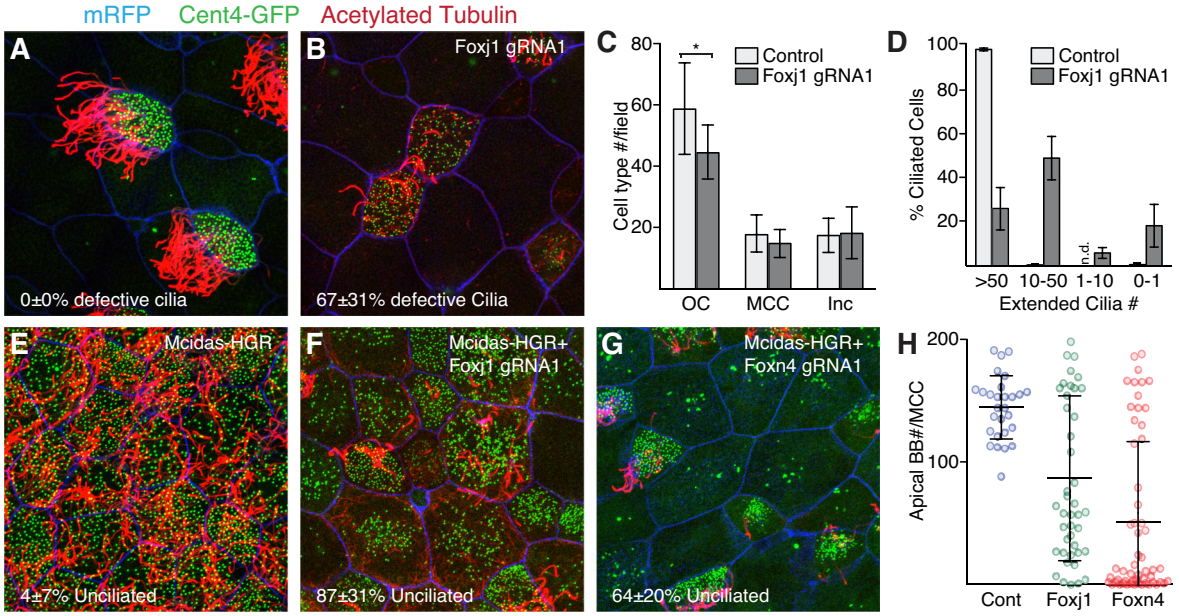

Fig. 3. Similar functions of Foxj1 and Foxn4 downstream of Multicilin. (A,B) Representative confocal images of the skin of stage 30 wild-type control (A) or Cas9/Foxj1^{gRNA1}-injected (B) embryos, where cell membranes (mRFP, blue), basal bodies (Centrin4-GFP, green) and cilia (acetylated tubulin, red) are labeled. The percentage of MCCs with cilia extension defects is indicated (±s.d.) based on scoring 12 fields from different embryos (n≥50 total cells). (C) The average number of MCCs, outer cells and putative ionocytes within a 0.085×0.085 mm field based on data from ≥12 embryos. Error bars indicate s.d. *P<0.05. (D) The percentage of MCCs extending >50, 10-50, 1-10 and 0 cilia in control and Cas9/Foxj1^{gRNA1}-injected embryos based on scoring ≥147 cells from eight to ten embryos. Error bars indicate s.d. n.d., not detected. (E-G) Confocal images of the skin of wild-type (E), Cas9/Foxj1^{gRNA1}-injected (F) or Cas9/Foxn4^{gRNA1}-injected (G) embryos, further injected with RNAs encoding Multicilin-HGR, mRFP (blue) or Centrin4-GFP (green). At stage 11.5, Multicilin activity was induced by treatment with Dex, and embryos were fixed at stage 26 and stained for cilia (red). The percentage of MCCs with cilia extension defects is indicated (±s.d.). (H) Scatter plot showing basal body number located within 1 µm of the apical surface of MCCs induced by Multicilin, in wild-type control (Cont), Cas9/Foxj1^{gRNA1}-injected (Foxj1) or Cas9/Foxn4^{gRNA1}-injected (Foxn4) embryos based on scoring 12 fields from different embryos. Bars indicate the mean and s.d.

Development (2016) 143, 4654-4664 doi:10.1242/dev.143859

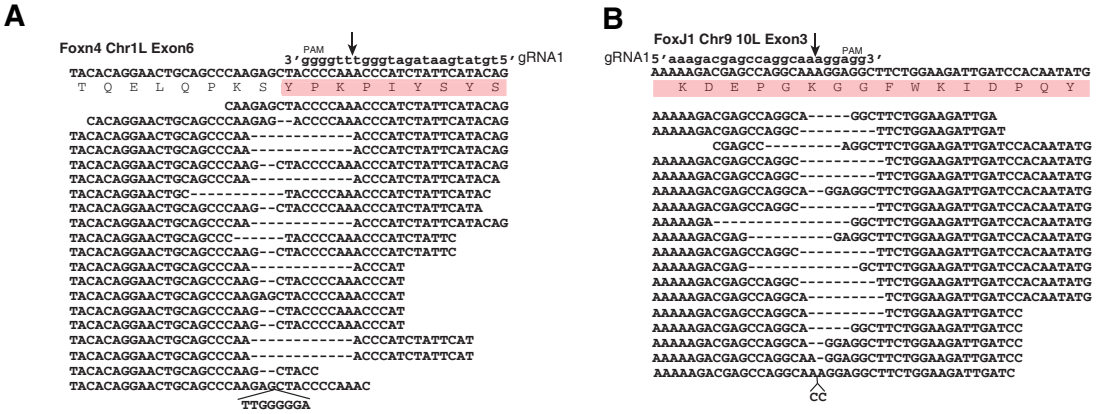

C

	Foxn4 gRNA1				Foxj1 gRNA1				Foxn4 MO			
	Rep1		Rep2		Rep1		Rep2		Foxn4		Foxj1	
	chr1s	chr1l	chr1s	chr1l	chr9_10s	chr9_10l	chr9_10s	chr9_10l	chr1s	chr1l	chr9_10s	chr9_10l
Wild Type Reads	0	2	0	2	3	1	4	3	28	24	78	75
Indel Reads	23	22	22	23	41	45	92	41	0	0	0	0

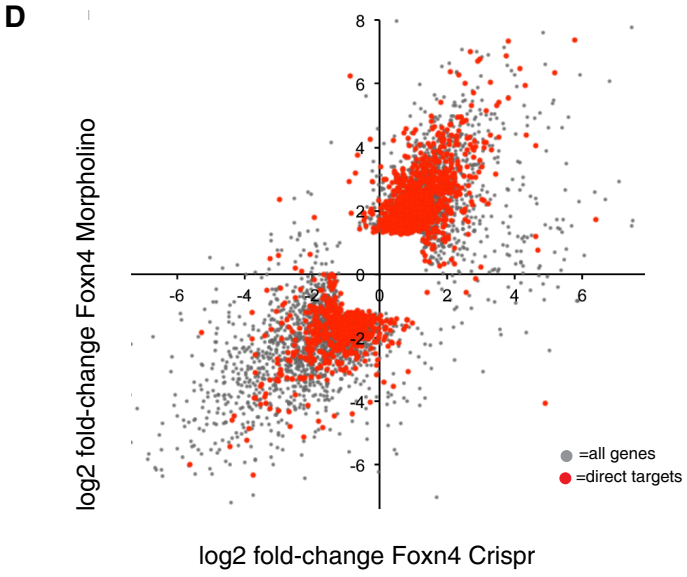

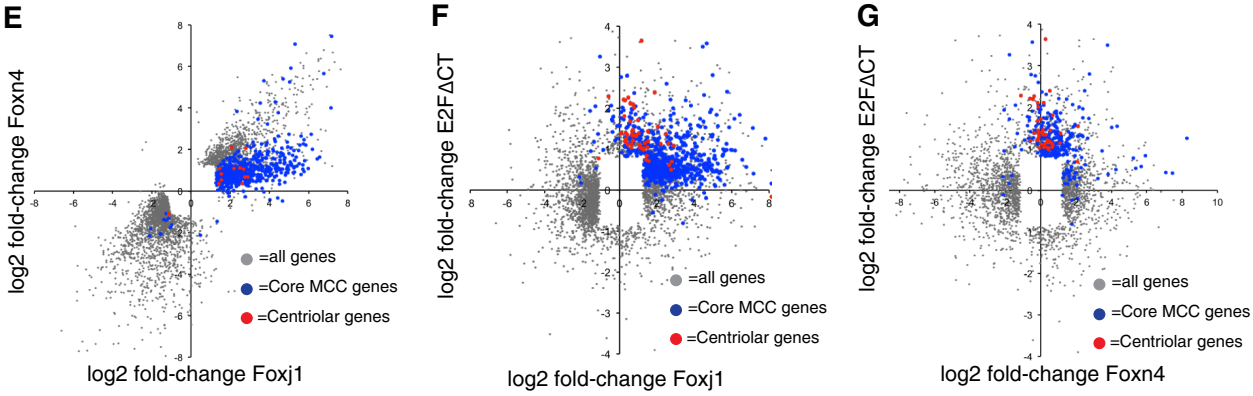

Fig. 4. See next page for legend.

Development (2016) 143, 4654-4664 doi:10.1242/dev.143859

Fig. 4. RNAseq analysis of *foxn4* and *foxj1* mutant phenotypes. (A,B) The *foxn4* and *foxj1* sequences targeted by the Foxn4 and Foxj1 gRNAs, on chromosomes Chr1l and Ch9_10L, respectively. The sequence and location of the gRNAs are indicated, along with the coding frame, and location of the forkhead domain (shaded in red). Beneath are 20 randomly chosen sequence reads that map to these regions in an RNAseq analysis of progenitors from embryos injected with Cas9 protein and Foxn4^{gRNA1} (A) or Foxj1^{gRNA1} (B). (C) The total wild-type and mutant sequence reads observed at the two homeologs of the *foxn4* and *foxj1* genes in replicate RNAseq analysis of embryos injected with Cas9 protein and Foxn4^{gRNA1}, Foxj1^{gRNA1}, or the Foxn4 morpholino as a control. (D) Scatter plot of genes based on a $\log_2$-fold change in expression (P<0.05) in RNAseq analysis of progenitors induced to undergo MCC differentiation with Multicilin, in the presence of a Foxn4 morpholino, or Cas9/Foxn4^{gRNA1}. Points in red are genes where Foxn4 binds directly within 1 kb of the TSS, based on ChIPseq analysis. (E-G) Scatter plots of genes based on $\log_2$-fold change in expression (P<0.05) in RNAseq analysis of progenitors induced to under MCC differentiation by Multicilin, in the presence and absence of E2f4ΔCT to disable the EDM complex (F,G), with Cas9/Foxj1^{gRNA1} to mutate *foxj1* (E,F) or with Cas9/Foxn4^{gRNA1} to mutate *foxn4* (E,G). All genes changes with P<0.05 are indicated in gray, MCC core genes defined in Quigley and Kintner (2016 preprint) are in blue, and genes associated with centriole biogenesis are in red (Ma et al., 2014).

in the phenotypes in *foxj1* and *foxn4* mutant MCCs, albeit mostly transient in one (*foxn4*) compared with the other (*foxj1*).

RNAseq analysis of Foxn4 versus Foxj1 morphants and mutants

We next exploited the accessibility of skin progenitors in *Xenopus* to carry out RNAseq analysis of the phenotypes produced using a morpholino versus nuclease-induced mutation. We isolated skin progenitors (animal caps) from stage 10.5 embryos, injected at the two-cell stage with RNA encoding inducible Multicilin alone, or after injection with the Foxn4 morpholino, with Cas9/Foxn4^{gRNA1} or with Cas9/Foxj1^{gRNA1}. Multicilin activity was induced at stage 11.5 and RNA isolated 9 h later, at the equivalent of stage 18, and subjected to RNAseq analysis. The RNAseq data were first used to estimate the efficacy of Cas9/CRISPR mutagenesis at the *foxn4* and *foxj1* genes in the pseudotetraploid *X. laevis* genome (Session et al., 2016). As predicted by the strong phenotypes, a large majority (>90%) of the reads mapping to the gene region targeted by the Foxn4 or Foxj1 gRNAs contained a mutation (mostly deletions and an occasional insertion) (Fig. 4A,B, Fig. S6). This mutation frequency is most likely to be an underestimate, in part because reads containing large deletions may fail to map, and transcripts with premature stop codons may be preferentially lost due to nonsense-mediated decay. By contrast, mutations were never detected in equivalent regions of the *foxn4* or *foxj1* genes in sequence reads obtained in the control (Foxn4 morpholino), in *foxn4* in the Foxj1 CRISPR/Cas9 sample, or in *foxj1* in the Foxn4 CRISPR/Cas9 sample (Fig. 4C).

To gain some estimate of whether each gRNA was prone to producing off-site mutation, we also examined all genomic positions with smaller regions of gRNA homology, up to five mismatches. Nearly all of the possible off-target positions identified were in non-exonic space (51/52) and the single possible exonic target of a Foxn4 gRNA, exon 3 of *cdh8*, showed no lesions in our RNAseq data (Table S2). Moreover, only one further position (a potential Foxj1 gRNA target) overlapped with a likely strong enhancer (H3K27ac^{+}), and no nearby genes were regulated in our RNAseq in ways different from their homologs, which did not harbor potential off-targets. Thus, although we did not have sufficient non-exonic sequencing coverage to determine if our gRNAs introduced indels at positions with a small number of mismatches, no predicted indel sites, if they exist, were likely to contribute meaningful differences to the expression of genes in our experiments.

We next analyzed the RNAseq data by plotting normalized gene expression obtained in Multicilin-activated progenitors in the presence of the Foxn4 morpholino versus that obtained in the presence of Cas9/Foxn4^{gRNA1} (Fig. 4D). Gene expression under the two conditions was strongly correlated, indicating that both methods result in similar changes in gene expression while failing to produce off-targets effects (Fig. 4D, Tables S3 and S4). *foxj1* mutants do not show a significant change in *foxn4* expression and vice versa, indicating that the two factors act independently and in parallel downstream of Multicilin (Fig. S7). We then compared changes in gene expression caused by Cas9/Foxj1^{gRNA1} (Table S5) versus Cas9/Foxn4^{gRNA1} (Table S4), or to changes found previously to occur when MCC differentiation was induced by Multicilin in the presence of an E2f4 mutant, called E2f4ΔCT, that disables the EDM complex (Ma et al., 2014) (Fig. 4E-G). Genes encoding centriolar components were more strongly inhibited during MCC differentiation by E2f4ΔCT (Ma et al., 2014) than by either *foxj1* or *foxn4* Cas9/CRISPR mutation, supporting the idea that the EDM complex, rather than the forkhead proteins, promotes centriole assembly during MCC differentiation (Fig. 4F,G). Also consistent with previous experiments, *foxj1* Cas9/CRISPR reduced a large fraction of the genes expressed in MCCs, consistent with its role as a major regulator of motile gene expression, but had much less of an effect on centriolar genes than the E2f4 mutant (Fig. 4E,F). Strikingly, *foxn4* Cas9/CRISPR mutations largely affected gene expression upregulated in MCCs that is also dependent on Foxj1 (Fig. 4E): we found no MCC genes regulated by Foxn4 that were not also regulated by Foxj1. Although several MCC genes regulated by Foxj1 were markedly dependent on Foxn4 (e.g. *cep68* and *cep164*), many of the genes upregulated by Foxj1 were also influenced by Foxn4 to a small degree (Fig. 4E, blue dots shifted upwards on the *y*-axis). Thus, these results indicate that Foxn4 is largely required during MCC differentiation to enhance the expression of Foxj1 targets – a few strongly and many weakly.

Foxn4 and Foxj1 have distinct genomic targets but may be recruited to MCC promoters by Rfx2

To determine direct targets of Foxn4, we performed ChIPseq analysis on progenitors injected with a tagged form of Foxn4 along with Multicilin to induce MCC differentiation, and compared these results with those previously obtained in a ChIPseq analysis of Foxj1 and Rfx2 (Quigley and Kintner, 2016 preprint; Chung et al., 2014) (Fig. 5A). Similar to the genome-wide binding observed for Foxj1 (Quigley and Kintner, 2016 preprint), Foxn4 rarely binds promoters but instead prefers binding to distal sites (Fig. S8). Given the similar phenotypes obtained by disrupting *foxj1* and *foxn4*, we predicted that both factors might bind together at a large number of positions, particularly at promoters of MCC genes. Most MCC promoters were bound by Foxn4, Foxj1, or both (702/950); most of these were bound by both factors, but relatively few were bound by Foxn4 alone (25/950) (Fig. 5B, Table S6). At promoters where Foxj1 and Foxn4 were co-bound, the number of sequence tags immunoprecipitated for each factor was high, suggesting robust binding (Fig. 5C).

De novo motif enrichment analysis of Foxn4-bound positions in the genome reveals further similarities to those previously found for Foxj1 (Quigley and Kintner, 2016 preprint). Like Foxj1, Foxn4 binding peaks are strongly enriched for the RFX motif, in addition to forkhead motifs (Fig. S9). Moreover, RFX motifs are found

Development (2016) 143, 4654-4664 doi:10.1242/dev.143859

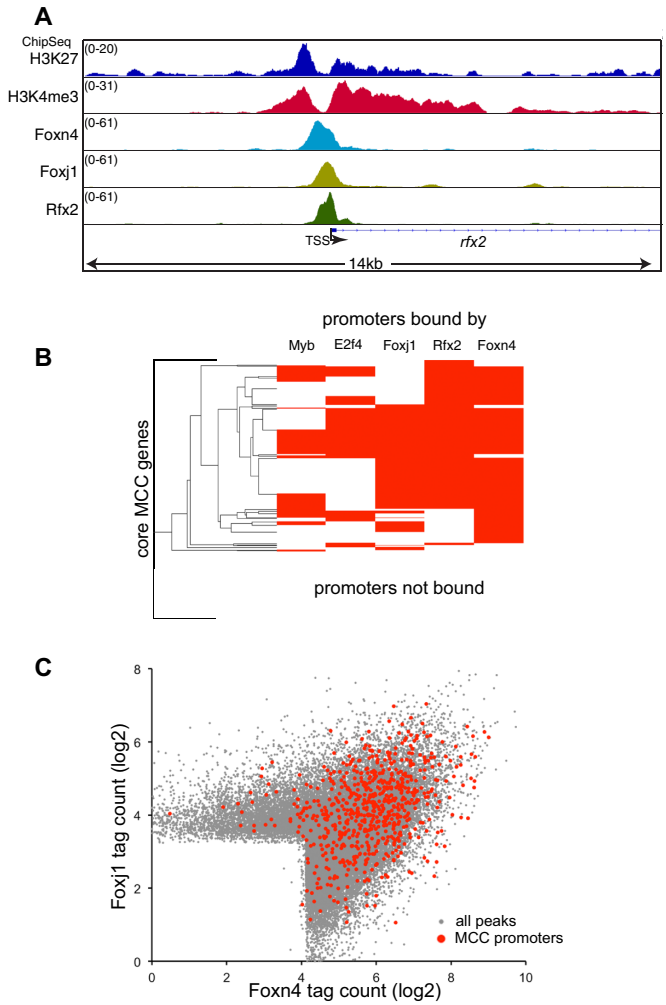

Fig. 5. Foxn4 binding in MCC promoters. ChIPseq analysis was carried out on a GFP-tagged form of Foxn4 expressed in epithelial progenitors along with Multicilin to induce MCC differentiation. Sequence reads obtained in this analysis were compared with that previously obtained for Rfx2 (Chung et al., 2014), E2f4 (Ma et al., 2014) or Foxj1 and various chromatin marks (Quigley and Kintner, 2016 preprint). (A) Genome browser screenshot of the *rfx2* promoter along with tag counts obtained in ChIPseq analysis of Foxn4, Rfx2, Foxj1 and chromatin marks as indicated. (B) The binding of different MCC transcription factors to the promoters of 950 genes that are markedly upregulated during MCC differentiation, based on previous extensive RNAseq analyses of skin progenitors (Quigley and Kintner, 2016 preprint). (C) Tag counts of Foxn4 and Foxj1 ChIPseq at all sites (gray) and all core MCC promoters (red) bound by either.

enriched within Foxn4 binding peaks at both distal and promoter sites, whereas forkhead motifs are found only at Foxn4 binding sites located distally (Fig. S10). Finally, Foxn4 binding at promoters typically occurred along with Rfx2 (Fig. S8, Table S3). Together, these results suggest that Foxn4 is likely to be bound to distal sites that are distinct from those bound by Foxj1, but is recruited in a similar manner as Foxj1 to MCC promoters via Rfx stabilization (Quigley and Kintner, 2016 preprint).

foxj1 and *foxn4* double mutants are extremely compromised in cilia extension

Functional overlap between Foxn4 and Foxj1 might also explain why MCC cilia extension in *foxn4* mutants largely recovers (Figs 2 and 3) and why most MCCs in *foxj1* mutants manage to extend a few cilia (Fig. 3B). To test this idea further, we injected embryos with both Foxn4 and Foxj1 gRNAs, and analyzed MCC differentiation at stage 28 (Fig. 6A-D). MCC formation occurred in double-mutant embryos at a similar rate as in single mutants, consistent with the idea that MCCs still initiate differentiation without Foxj1 and Foxn4 (Fig. 6E). However, most of the MCCs in the double mutants completely failed to extend any cilia (Fig. 6D), even though centriole expansion, based on labeling with Centrin4-GFP, still occurred but remained deep in the cytoplasm (Fig. 6D,F). Thus, Foxn4 and Foxj1 are likely to act in a partially overlapping manner to promote basal body docking and cilia extension during MCC differentiation.

Foxj1 but not Foxn4 is required for motile ciliogenesis in the LRO

A single motile cilium forms on cells within the gastrocoel roof plate (GRP) of the *Xenopus* embryo, a segment of epithelium called the LRO where the left-right axis is broken by a leftward flow (Blum et al., 2009; Walentek et al., 2012). Since Foxj1 is necessary and sufficient to form a single motile cilium (Stubbs et al., 2008), Foxn4 might be dispensable within the LRO. Indeed, as shown previously using a morpholino (Stubbs et al., 2008), loss of *foxj1* using Cas9/CRISPR mutagenesis (Fig. 7A,B) results in abnormal ciliogenesis in the GRP: cilia length is dramatically reduced and cilia fail to position to the posterior side of the cell (Fig. 7D,E), suggesting that they have lost their motile character. By contrast, in Cas9/Foxn4^{gRNA1}-injected embryos (Fig. 7A,C), cilia formation on the GRP appeared normal (Fig. 7D,E), even though the same batch of injected embryos at later stages show defects in MCCs. These results are in line with the idea that Foxn4 is required as a co-factor for motile cilia formation only in MCCs, presumably to deal with the transcriptional load required to undergo multiple ciliation.

DISCUSSION

Foxn4 expression is strongly associated with MCC differentiation in different tissues and in different species, most likely as a direct target of Multicilin-mediated transcriptional activation. Initial attempts to characterize Foxn4 function in the mouse lung using conditional mutants failed to detect a gross phenotype in the proximal airways, in that markers for various cell types, including MCCs, were not detectably changed (Li and Xiang, 2011). Our results are largely consistent with those in the mouse, in that knocking down or removing Foxn4 function in the *Xenopus* skin does not lead to detectable alterations in cell fate. Nonetheless, closer examination of the Foxn4 phenotypes in *Xenopus* reveals a significant delay and incomplete MCC differentiation that could have easily been missed in analyzing the mouse mutant phenotype. Thus, Foxn4 needs to be re-examined in mouse MCCs, especially as partial genetic redundancy in the pathways that drive MCC differentiation has become a recurring theme. For example, mutations in two crucial regulators of MCC differentiation, namely *Ccno* and *Myb*, cause severe defects in MCC differentiation in the mouse lung initially but also eventually recover, at least superficially, over time (Funk et al., 2015; Tan et al., 2013).

foxn4 mutant phenotypes

Concerns have been raised about morpholino-based phenotypes in zebrafish since many are not recapitulated in F1 mutants generated by nuclease-mediated mutagenesis (Kok et al., 2015). The reason for this discrepancy is not fully understood, but could be due to the various limitations inherent to either approach (Blum et al., 2015; Stainier et al., 2015). On the one hand, morpholinos are known to

Development (2016) 143, 4654-4664 doi:10.1242/dev.143859

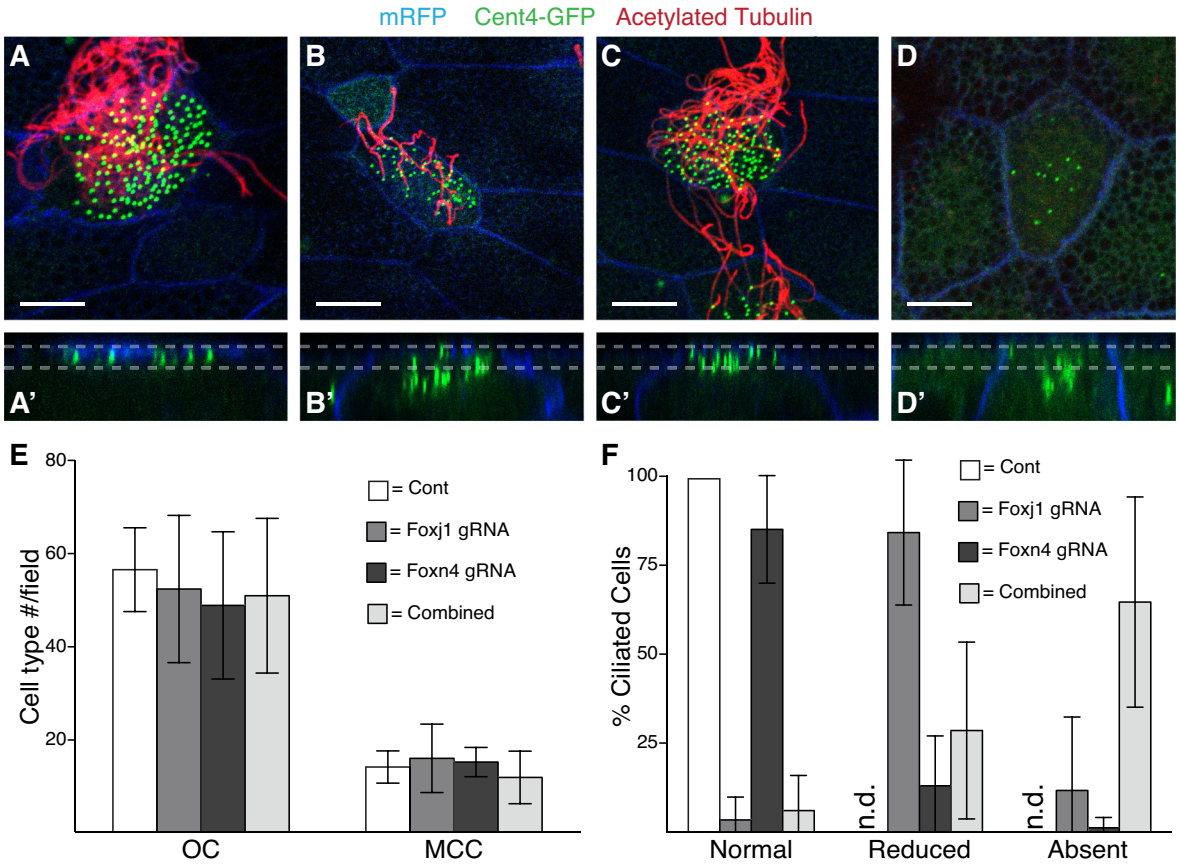

Fig. 6. MCC differentiation in *foxn4* and *foxj1* double mutants. (A-D) Shown are representative confocal images of the skin in embryos that were injected with Cas9/Foxj1^{gRNA1} (B), Cas9/Foxn4^{gRNA1} (C) or both (D), or left uninjected as control (A). Cell membranes are labeled with mRFP (blue), basal bodies with Centrin4-GFP (green) and cilia with acetylated tubulin antibody (red). (A-D′) *z*-sections, with dashed lines indicating the apical location of docked basal bodies in control MCCs. Scale bars: 10 µm. (E) The frequency of all MCCs (scored based on centriole expansion, docked or undocked) and outer cells in the skin of embryos injected with Cas9 and gRNAs as indicated. No values differ significantly from control embryos. (F) MCCs in embryos injected with Cas9 and gRNAs as indicated were scored based on wild-type cilia extension (as in A), reduced cilia (as in B) or absent cilia (as in D). (E,F) Data are based on >19 randomly chosen fields (0.13×0.13 mm) from different embryos. n.d., not detected. Error bars indicate s.d.

have off-targets effects that can be difficult to control for, even by carrying out a rescue experiment. On the other hand, nuclease-induced mutations are not necessarily nulls, given the possibility of exon skipping, and the use of alternative transcriptional/translational start sites that can bypass the mutation to produce a functional protein. Loss-of-function phenotypes can also be masked by the upregulation of compensatory pathways (Rossi et al., 2015). Our analysis of the morpholino and nuclease-generated *foxn4* mutant phenotypes, however, indicates a close correspondence in terms of developmental timing, cellular features, and gene expression changes revealed by RNAseq analysis, suggesting that off-site targets are unlikely to be major contributors to the phenotypes reported here. The similar phenotypes generated using the two approaches also provide considerable confidence that certain features are not artifacts. For example, the recovery of the MCC phenotype in many cells in Foxn4 morphants is unlikely to be due to a depletion of the morpholino over time since the *foxn4* Cas9/CRISPR mutants show the same recovery. Conversely, the morphant phenotypes support the idea that the efficacy of the nuclease-mediated mutagenesis in F0 animals can be high enough to target all four alleles and generate null phenotypes. gRNAs against the same gene can vary enormously in their phenotypic efficacy (Fig. 2), making a nuclease-mediated approach in *X. laevis* F0 embryos challenging in terms of creating complete nulls. Since the highly efficient gRNAs used here all targeted sequences encoding the DNA-binding domain, this approach might have focused on highly conserved regions where essentially any deletion would be sufficient to disable protein function.

Fox transcription factors in MCC differentiation

The developmental mechanisms that underlie robust gene expression during the differentiation of many cell types are still poorly understood. The differentiation of MCCs in the *Xenopus* skin provides a window into these mechanisms, since it occurs synchronously but with a characteristic temporal sequence, requires a burst in the expression of ∼950 genes that encode the molecular complexes that underlie multiple motile ciliation, and produces an outcome (e.g. cilia) that can be readily scored quantitatively. Our results suggest that Foxn4 ensures robust gene expression during MCC differentiation since, in its absence, cilia formation is markedly delayed and fails to go to completion in some cells. As one of the first targets of the EDM complex, Foxn4 therefore appears to function early in MCC differentiation to shape a robust transcriptional output required for the timely formation of motile cilia, in a cell context where hundreds of such structures need to form.

Foxn4 function largely follows that previously assigned to Foxj1, in that Foxn4 is required to potentiate the expression of many

Development (2016) 143, 4654-4664 doi:10.1242/dev.143859

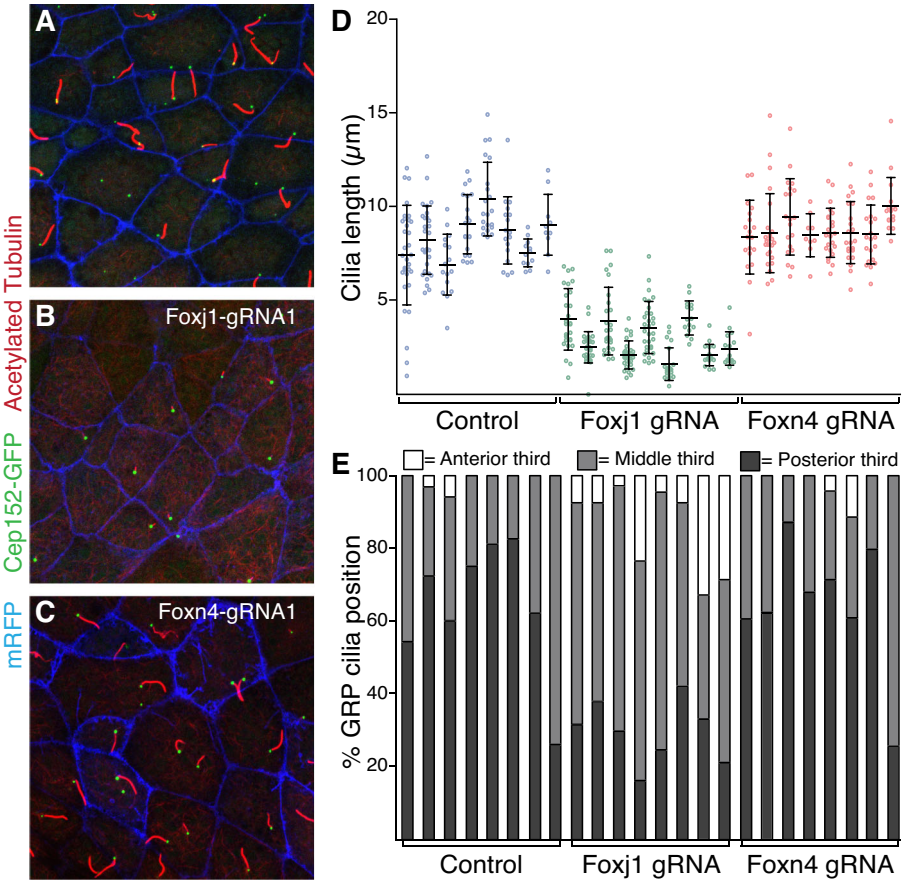

Fig. 7. GRP cilia formation in *foxn4* and *foxj1* mutant embryos. (A-C) Embryos were injected with Foxj1^{gRNA1} or Foxn4^{gRNA1} along with Cas9 protein, followed by RNA encoding mRFP (blue) or Cep152-GFP (green) to label membranes and centrioles, respectively. At stage 17/18, the dorsal tissue was dissected away to expose the GRP, fixed, stained for cilia (red) and imaged by confocal microscopy. Typical confocal images are shown of GRP cells in control (A), Cas9/Foxj1^{gRNA1}-injected (B) or Cas9/Foxn4^{gRNA1}-injected (C) embryos. Anterior is up. (D) Scatter plot showing length of GRP cilia in cells from individual embryos injected as indicated. Mean and s.d. are indicated. (E) Cilia positioning in cells along the anteroposterior axis in the GRP was measured in embryos injected as indicated. Each bar shows data from individual GRPs based on data obtained from 10-30 cells, with the percentage of cells with cilia located in the anterior, middle or posterior third indicated. Most GRP cells have a posteriorly localized cilium in control (69±11%) and Cas9/Foxn4^{gRNA1}-injected (69±9%) embryos, but not in Cas9/Foxj1^{gRNA1}-injected embryos (29±9%; P=9×10^{-7}).

Foxj1-regulated genes weakly and a subset of the Foxj1 target genes strongly. Which of these genes account for the cilia phenotypes observed in *foxn4* mutants will require further investigation, especially since many of the genes strongly downregulated in *foxn4* mutants remain poorly annotated. Like Foxj1 (Quigley and Kintner, 2016 preprint), Foxn4 binding appears to occur directly at distal enhancers but is then recruited to MCC promoters via Rfx2, thus providing an alternative means of recruiting additional enhancers to MCC genes to promote gene expression, perhaps during the early phases of MCC differentiation. In addition, like Foxj1, ectopic expression of Foxn4 is sufficient to drive the formation of long ectopic cilia in cells that are not normally ciliated. We further note that in mice, *Foxn4* expression, like that of *Mcidas*/*Gemc1* (*Gmnc*), appears transient in MCCs (Li and Xiang, 2011), whereas *Foxj1* expression is known to persist in fully differentiated cells, presumably due to a positive-feedback loop on its own expression. Thus, Foxn4 might be crucial during a phase when multiple motile cilia are initially assembled as progenitors differentiate, while Foxj1 is not only involved in their assembly but also in their maintenance in a fully functioning cell. Further dissection of genes that are differentially regulated by Foxn4 and Foxj1 could therefore provide important insights into how cilia are first assembled and then maintained in the long-lived MCC.

MATERIALS AND METHODS

Embryos, RNA synthesis and microinjections

Xenopus laevis embryos were prepared by *in vitro* fertilization using standard protocols (Sive et al., 1998). Injections of synthetic RNAs or a Foxn4 morpholino were carried out at the 2- to 4-cell stage, targeting all four quadrants of the animal pole and typically using 0.1 to 5.0 ng/embryo of RNA and 5 picomoles of morpholino. Morpholinos (Table S1) target the initiation ATG of *foxn4* on both chromosomes 1S and 1L. Embryos were typically allowed to develop at 16°C overnight until gastrulation was complete, and then at room temperature.

RNA synthesis and templates

Capped synthetic RNAs were generated *in vitro* using previously described methods (Stubbs et al., 2008). Templates for generating RNA encoding Multicilin-HGR, membrane-RFP (mRFP), Centrin4-GFP, Tsga10-GFP, Chibby-GFP, Clamp-GFP and Hyls1-GFP have been described previously (Chien et al., 2015, 2013; Stubbs et al., 2012). The template for expressing an inducible Foxn4 was generated by isolating a *foxn4* cDNA using PCR primers (Table S1), sequencing, and cloning in-frame into a CS2 vector containing the ligand-binding domain from the human glucocorticoid receptor (Stubbs et al., 2012).

CRISPR gRNAs for targeting *foxn4* and *foxj1* were generated *in vitro* from templates generated by PCR, as described previously (Bhattacharya et al., 2015). Briefly, cDNA sequences for *foxj1* and *foxn4* obtained from Xenbase were searched using Crisprdirect (http://crispr.dbcls.jp) for a 5′ GG-N(20) target sequence (Table S1, Fig. 4) that was conserved in both forms encoded by the S and L chromosomes in *X. laevis*, that would produce a cleavage disrupting sequences encoding the forkhead domain, and that would minimize potential predicted off-site targets (Fig. 4). This sequence was incorporated into a PCR primer that starts with a 5 bp stabilization sequence, the T7 promoter and a 20 bp overlap with a universal Cas9 PCR primer as described (Bhattacharya et al., 2015). PCR conditions for template generation followed those of Bhattacharya et al. (2015) except that exTAQ (Takara Clontech) was used as the polymerase and 30 s was used for annealing. PCR products were column purified and used to generate gRNA using T7 polymerase (Promega) following the manufacturer's protocol and buffer conditions. gRNAs were treated with DNase I (RNase free, Promega), phenol-chloroform extracted, and ethanol precipitated, once with ammonium acetate and then with sodium acetate as the salt. gRNAs were resuspended in 15-20 µl DEPC-treated water (typical yield 2.5 µg).

Development (2016) 143, 4654-4664 doi:10.1242/dev.143859

Cas9 protein [2.5 µl (PNA-Bio #CP01) at 1 µg/µl] along with a gRNA (2.5 µl) were allowed to assemble on ice for 15 min, and then injected once (1-5 nl) into the animal pole 20-40 min after fertilization.

Immunohistochemistry

MCC differentiation was assessed in embryos using confocal microscopy to visualize cell boundaries marked with mRFP, basal bodies marked with Hyls1-GFP, Chibby-GFP, Tsga10-GFP or Clamp-GFP, and cilia stained with mouse anti-acetylated tubulin (Sigma, T6793; 1:1000) followed by a Cy5-conjugated secondary antibody (Jackson Labs, 715-605-150; 1:500). Embryos were processed by a 10 min fixation in 3.7% formaldehyde, 0.25% glutaraldehyde in PBT (PBS with 0.1% Triton X-100), followed by antibody staining. Embryos were mounted in PVA with DABCO (Sigma, D27802) and imaged on a Zeiss LSM710 confocal microscope.

Data for basal body counting were typically collected from two or three randomly chosen fields from five to ten embryos per sample. Cells with undocked basal bodies were scored based on the presence of a significant number of basal bodies located 1 µm below the apical surface. Cells with defective cilia were scored based on the presence of severely shortened, reduced numbers of cilia. Cell type quantification in each experiment used data based on ten fields from ten different embryos chosen at random. Cell type number, basal body number and cell size were quantified using ImageJ software. Statistical significance was assessed in all experiments using two-tailed *t*-tests.

RNAseq analysis of *foxn4* and *foxj1* mutants

RNA was isolated from epidermal progenitors (animal caps) that were dissected from stage 10 embryos, injected as above with the Foxn4 morpholino, or with Cas9 protein and Foxn4 or Foxj1 gRNAs, followed by injection at the 4-cell stage with RNA encoding Multicilin-HGR, again targeting all four animal quadrants. Wild-type embryos injected with just Multicilin-HGR served as the control. Animal caps were cultured at 22°C in 0.5×MMR (Sive et al., 1998), treated with dexamethasone (1 µM) at stage 11 to induce Multicilin-HGR, and harvested 9 h later, using the proteinase K method, followed by phenol-chloroform extractions, lithium precipitation, treatment with RNase-free DNase, and a second series of phenol-chloroform extractions and ethanol precipitation (Ma et al., 2014).

RNAseq libraries were constructed with Illumina TruSeq RNA Sample Preparation Kit v2 according to the manufacturer's instructions and sequenced on a HiSeq 2000 or 2500 at 1×50 or 1×100 bp to a depth of 20-40 million reads. Each RNAseq condition was performed in duplicate, using animal caps isolated from different females. FASTQ reads were aligned to the *X. laevis* transcriptome, MayBall version (http://daudin.icmb.utexas.edu/), with RNA-STAR (Dobin et al., 2013). Aligned reads were then counted with eXpress (Roberts and Pachter, 2011), and DESeq (Anders and Huber, 2010) was then used to normalize, estimate dispersion, and test differential expression using rounded raw counts from eXpress.

ChIPseq libraries

Because ChIP-grade antibodies are generally not available that recognize *Xenopus* proteins, we tagged Foxn4 with GFP (which remained active for inducing ectopic cilia) and injected embryos with a RNA transcript encoding this construct. Samples were prepared for ChIP using previously described methods (Blythe et al., 2009) with the following modifications: ~250 animal caps from injected embryos were fixed for 30 min in 1% formaldehyde, and chromatin was sheared on a BioRuptor (30 min; 30 s on and 2 min off at highest power setting). Tagged Foxn4 with associated chromatin was immunoprecipitated with antibodies directed against GFP (Invitrogen, A11122, lot no. 1296649). Recovered DNA fragments were then polished (New England Biolabs, End Repair Module), adenylated (New England Biolabs, Klenow fragment, 3′-5′ exo- and dA-tailing buffer), ligated to standard Illumina indexed adapters (TruSeq version 2), PCR amplified (New England Biolabs, Phusion or Q5, 16 cycles) and sequenced on an Illumina platform.

ChIPseq informatics

ChIPseq reads from this study were mapped to the interim *X. laevis* genome build v7.1 (Session et al., 2016) with Bowtie 2 (Langmead and Salzberg, 2012) and peaks called with HOMER (Heinz et al., 2010) using input as background. Peak positions were annotated relative to known exons (MayBall gene models; http://daudin.icmb.utexas.edu/), with promoters defined as being ±1 kb around the transcription start site (TSS). Peak sequences were interrogated for *de novo* motif enrichment with HOMER (Heinz et al., 2010) and MCC promoters (MCC gene list from Quigley and Kintner, 2016 preprint) were clustered (based on whether they were bound/not bound) with Cluster 3.0 and visualized with Java Treeview (v1.1.6r). Tags or motifs were counted at peak positions with HOMER and plotted with Excel (Microsoft).

Acknowledgements

We thank Dr Seongjae Kim for comments on the manuscript.

Competing interests

The authors declare no competing or financial interests.

Author contributions

E.P.C. and C.K. conceived and performed experiments, and wrote the manuscript. C.K. secured funding. I.K.Q. performed genomic experiments, carried out the bioinformatics analysis, and reviewed and edited the manuscript.

Funding

The work reported here was supported by a National Institutes of Health grant [RO1-GM076507] to C.K. Deposited in PMC for release after 12 months.

Data availability

ChIPseq and RNAseq sequence reads are deposited at NCBI Gene Expression Omnibus with accession number GSE89271.

Supplementary information

Supplementary information available online at
http://dev.biologists.org/lookup/doi/10.1242/dev.143859.supplemental

References

Anders, S. and Huber, W. (2010). Differential expression analysis for sequence count data. *Genome Biol.* **11**, R106.

Arbi, M., Pefani, D. E., Kyrousi, C., Lalioti, M. E., Kalogeropoulou, A., Papanastasiou, A. D., Taraviras, S. and Lygerou, Z. (2016). GemC1 controls multiciliogenesis in the airway epithelium. *EMBO Rep.* **17**, 400-413.

Bhattacharya, D., Marfo, C. A., Li, D., Lane, M. and Khokha, M. K. (2015). CRISPR/Cas9: an inexpensive, efficient loss of function tool to screen human disease genes in Xenopus. *Dev. Biol.* **408**, 196-204.

Blum, M., Beyer, T., Weber, T., Vick, P., Andre, P., Bitzer, E. and Schweickert, A. (2009). Xenopus, an ideal model system to study vertebrate left-right asymmetry. *Dev. Dyn.* **238**, 1215-1225.

Blum, M., De Robertis, E. M., Wallingford, J. B. and Niehrs, C. (2015). Morpholinos: antisense and sensibility. *Dev. Cell* **35**, 145-149.

Blythe, S. A., Reid, C. D., Kessler, D. S. and Klein, P. S. (2009). Chromatin immunoprecipitation in early Xenopus laevis embryos. *Dev. Dyn.* **238**, 1422-1432.

Brody, S. L., Yan, X. H., Wuerffel, M. K., Song, S.-K. and Shapiro, S. D. (2000). Ciliogenesis and left-right axis defects in forkhead factor HFH-4-null mice. *Am. J. Respir. Cell Mol. Biol.* **23**, 45-51.

Brooks, E. R. and Wallingford, J. B. (2014). Multiciliated cells. *Curr. Biol.* **24**, R973-R982.

Chien, Y.-H., Werner, M. E., Stubbs, J., Joens, M. S., Li, J., Chien, S., Fitzpatrick, J. A. J., Mitchell, B. J. and Kintner, C. (2013). Bbof1 is required to maintain cilia orientation. *Development* **140**, 3468-3477.

Chien, Y.-H., Keller, R., Kintner, C. and Shook, D. R. (2015). Mechanical strain determines the axis of planar polarity in ciliated epithelia. *Curr. Biol.* **25**, 2774-2784.

Choksi, S. P., Lauter, G., Swoboda, P. and Roy, S. (2014). Switching on cilia: transcriptional networks regulating ciliogenesis. *Development* **141**, 1427-1441.

Chung, M.-I., Kwon, T., Tu, F., Brooks, E. R., Gupta, R., Meyer, M., Baker, J. C., Marcotte, E. M. and Wallingford, J. B. (2014). Coordinated genomic control of ciliogenesis and cell movement by RFX2. *eLife* **3**, e01439.

Dammermann, A., Pemble, H., Mitchell, B. J., McLeod, I., Yates, J. R., III, Kintner, C., Desai, A. B. and Oegema, K. (2009). The hydrolethalus syndrome protein HYLS-1 links core centriole structure to cilia formation. *Genes Dev.* **23**, 2046-2059.

Dobin, A., Davis, C. A., Schlesinger, F., Drenkow, J., Zaleski, C., Jha, S., Batut, P., Chaisson, M. and Gingeras, T. R. (2013). STAR: ultrafast universal RNA-seq aligner. *Bioinformatics* **29**, 15-21.

Funk, M. C., Bera, A. N., Menchen, T., Kuales, G., Thriene, K., Lienkamp, S. S., Dengjel, J., Omran, H., Frank, M. and Arnold, S. J. (2015). Cyclin O (Ccno)

functions during deuterosome-mediated centriole amplification of multiciliated cells. *EMBO J.* **34**, 1078-1089.
Guo, X., Zhang, T., Hu, Z., Zhang, Y., Shi, Z., Wang, Q., Cui, Y., Wang, F., Zhao, H. and Chen, Y. (2014). Efficient RNA/Cas9-mediated genome editing in Xenopus tropicalis. *Development* **141**, 707-714.
Heinz, S., Benner, C., Spann, N., Bertolino, E., Lin, Y. C., Laslo, P., Cheng, J. X., Murre, C., Singh, H. and Glass, C. K. (2010). Simple combinations of lineage-determining transcription factors prime cis-regulatory elements required for macrophage and B cell identities. *Mol. Cell* **38**, 576-589.
Hoh, R. A., Stowe, T. R., Turk, E. and Stearns, T. (2012). Transcriptional program of ciliated epithelial cells reveals new cilium and centrosome components and links to human disease. *PLoS ONE* **7**, e52166.
Kok, F. O., Shin, M., Ni, C.-W., Gupta, A., Grosse, A. S., van Impel, A., Kirchmaier, B. C., Peterson-Maduro, J., Kourkoulis, G., Male, I. et al. (2015). Reverse genetic screening reveals poor correlation between morpholino-induced and mutant phenotypes in zebrafish. *Dev. Cell* **32**, 97-108.
Kyrousi, C., Arbi, M., Pilz, G.-A., Pefani, D.-E., Lalioti, M.-E., Ninkovic, J., Gotz, M., Lygerou, Z. and Taraviras, S. (2015). Mcidas and GemC1 are key regulators for the generation of multiciliated ependymal cells in the adult neurogenic niche. *Development* **142**, 3661-3674.
Langmead, B. and Salzberg, S. L. (2012). Fast gapped-read alignment with Bowtie 2. *Nat. Methods* **9**, 357-359.
Li, S. and Xiang, M. (2011). Foxn4 influences alveologenesis during lung development. *Dev. Dyn.* **240**, 1512-1517.
Ma, L., Quigley, I., Omran, H. and Kintner, C. (2014). Multicilin drives centriole biogenesis via E2f proteins. *Genes Dev.* **28**, 1461-1471.
Nemajerova, A., Kramer, D., Siller, S. S., Herr, C., Shomroni, O., Pena, T., Gallinas Suazo, C., Glaser, K., Wildung, M., Steffen, H. et al. (2016). TAp73 is a central transcriptional regulator of airway multiciliogenesis. *Genes Dev.* **30**, 1300-1312.
Pan, J.-H., Adair-Kirk, T. L., Patel, A. C., Huang, T., Yozamp, N. S., Xu, J., Reddy, E. P., Byers, D. E., Pierce, R. A., Holtzman, M. J. et al. (2014). Myb permits multilineage airway epithelial cell differentiation. *Stem Cells* **32**, 3245-3256.
Quigley, I. K. and Kintner, C. (2016). Rfx2 stabilizes Foxj1 binding at chromatin loops to enable multiciliated cell gene expression. *bioRxiv*, doi: 10.1101/085571.
Roberts, A. and Pachter, L. (2011). RNA-Seq and find: entering the RNA deep field. *Genome Med.* **3**, 74.
Rossi, A., Kontarakis, Z., Gerri, C., Nolte, H., Hölper, S., Krüger, M. and Stainier, D. Y. R. (2015). Genetic compensation induced by deleterious mutations but not gene knockdowns. *Nature* **524**, 230-233.
Session, A. M., Uno, Y., Kwon, T., Chapman, J. A., Toyoda, A., Takahashi, S., Fukui, A., Hikosaka, A., Suzuki, A., Kondo, M. et al. (2016). Genome evolution in the allotetraploid frog Xenopus laevis. *Nature* **538**, 336-343.
Sive, H., Grainger, R. M. and Harland, R. M. (1998). *The Early Development of Xenopus laevis: A Laboratory Manual*. Plainview, NY: Cold Spring Harbor Press.
Stainier, D. Y. R., Kontarakis, Z. and Rossi, A. (2015). Making sense of anti-sense data. *Dev. Cell* **32**, 7-8.
Stubbs, J. L., Oishi, I., Izpisúa Belmonte, J. C. and Kintner, C. (2008). The forkhead protein Foxj1 specifies node-like cilia in Xenopus and zebrafish embryos. *Nat. Genet.* **40**, 1454-1460.
Stubbs, J. L., Vladar, E. K., Axelrod, J. D. and Kintner, C. (2012). Multicilin promotes centriole assembly and ciliogenesis during multiciliate cell differentiation. *Nat. Cell Biol.* **14**, 140-147.
Tan, F. E., Vladar, E. K., Ma, L., Fuentealba, L. C., Hoh, R., Espinoza, F. H., Axelrod, J. D., Alvarez-Buylla, A., Stearns, T., Kintner, C. et al. (2013). Myb promotes centriole amplification and later steps of the multiciliogenesis program. *Development* **140**, 4277-4286.
Terre, B., Piergiovanni, G., Segura-Bayona, S., Gil-Gomez, G., Youssef, S. A., Attolini, C. S.-O., Wilsch-Brauninger, M., Jung, C., Rojas, A. M., Marjanovic, M. et al. (2016). GEMC1 is a critical regulator of multiciliated cell differentiation. *EMBO J.* **35**, 942-960.
Treutlein, B., Brownfield, D. G., Wu, A. R., Neff, N. F., Mantalas, G. L., Espinoza, F. H., Desai, T. J., Krasnow, M. A. and Quake, S. R. (2014). Reconstructing lineage hierarchies of the distal lung epithelium using single-cell RNA-seq. *Nature* **509**, 371-375.
Walentek, P., Beyer, T., Thumberger, T., Schweickert, A. and Blum, M. (2012). ATP4a is required for Wnt-dependent Foxj1 expression and leftward flow in Xenopus left-right development. *Cell Rep.* **1**, 516-527.
Zhou, F., Narasimhan, V., Shboul, M., Chong, Y. L., Reversade, B. and Roy, S. (2015). Gmnc is a master regulator of the multiciliated cell differentiation program. *Curr. Biol.* **25**, 3267-3273.